Antenna Pattern Impact on MIMO OTA Testing

Fan, Wei; Nielsen, Jesper Ødum; Franek, Ondrej; Carreño, Xavier; S. Ashta, Jagjit ; B. Knudsen, Mikael; Pedersen, Gert Frølund

Published in:
I E E E Transactions on Antennas and Propagation

DOI (link to publication from Publisher):
10.1109/TAP.2013.2279805

Publication date:
2013

Document Version
Early version, also known as pre-print

Antenna Pattern Impact on MIMO OTA Testing

Wei Fan, Jesper Ø. Nielsen, Ondrej Franek, Xavier Carreño, Jagjit S. Ashta, Mikael B. Knudsen and Gert F. Pedersen

***Abstract*—This paper investigates the impact of the DUT antenna pattern on the test area performance for multi-probe based MIMO OTA setup in terms of received voltage and spatial correlation. The plane wave synthesis (PWS) technique has been proposed for vertical polarization in the literature, where the goal is to approximate plane waves with arbitrary directions. The received voltage at the antenna terminal depends on the antenna radiation pattern and the impinging plane waves. A novel closed form technique to reproduce the received voltage with arbitrary incoming plane waves based on trigonometric interpolation is presented. The proposed technique provides a closed form solution for the PWS when the probe ring radius is infinite. The proposed technique shows that the impact of the antenna pattern on the induced received voltage accuracy is ruled by Nyquist sampling theory. Furthermore, the impact of the antenna pattern on spatial correlation accuracy for prefaded signal synthesis (PFS) technique is investigated as well. Simulation and measurement results show that the number of required probes depend directly on the DUT antenna pattern. To test realistic DUTs with higher variations in directivity, we need more probes to maintain the same received voltage and spatial correlation accuracy level.**

I. Introduction

Multiple-input multiple-output (MIMO) technology is a key factor for achieving high data rate for wireless technologies such as LTE and LTE-Advanced. Mobile manufacturers and cellular operators are pushing for standard test methods to evaluate MIMO device performance. As a promising solution to evaluate MIMO device performance in realistic conditions in the lab, MIMO over the air (OTA) testing has attracted huge attention from both industry and academia [1]. Standardization work for the development of the MIMO OTA test methods is ongoing in CTIA, 3GPP and COST IC1004 [1]. One promising candidate is the multi-probe anechoic chamber based method.

The major challenge for MIMO OTA testing with the multi-probe method is to emulate a realistic environment which accurately reflects the real wireless propagation environment. Mainly two channel emulation techniques have been proposed for multi-probe based MIMO OTA setups. One technique is the plane wave synthesis (PWS) technique reported in [2]–[6]. The basic idea of the PWS technique is that static plane waves with arbitrary impinging angle of arrivals (AoAs) can be created inside the test area by selecting appropriate complex weights for the probes. Desired radio channels inside the test area can be formed based on superposition of a plurality of plane waves as detailed in [2], [3]. The other technique is named the prefaded signal synthesis (PFS) technique [2] and has been adopted in several commercial tools [7]–[9]. The essence of this technique is to allocate proper power weights to the probes to reproduce the channel desired spatial characteristics at the receiver (Rx) side [7].

The test area is the geometrical area inside which the DUT is located during the measurement. Acceptable error levels are defined for the channel emulation to ensure that the target propagation environment is reproduced around the DUT with certain accuracy. The required number of probes is a key issue related to the multi-probe anechoic chamber solution. It is generally assumed that the number of probes depends on the test area size, the center frequency, the channel model, the OTA probe angular locations, and the acceptable error level [2], [6], while the DUT antenna pattern has been considered irrelevant. The above-mentioned two techniques generally assume that:

- For the PWS technique, the goal is to approximate plane waves inside the test area. However, what matters is whether we can reproduce the desired received voltage with the multiple probes. The difference between target received voltage, assuming ideal impinging plane waves with arbitrary AoAs, and the induced received voltage, with waves radiated from the multiple probes impinging the DUT, has not been investigated. The resulting received voltage accuracy depends on the antenna pattern, as demonstrated in this paper.
- For the PFS technique, the difference between the target spatial correlation and the emulated spatial correlation of the ideal omnidirectional antennas are used to determine the number of required probes. However, what matters is whether we can reproduce the spatial correlation of the received signals at the antenna output.

The main contributions of this paper lie in the following aspects:

- An optimization technique for PWS of horizontal polarization is introduced. Simulation results show that the difference between the complex weights for the two polarizations depends on the ratio between test area radius and OTA ring radius r/R and the complex weights are practically the same for large R cases.
- A novel closed form technique to reproduce the target received voltage based on trigonometric interpolation (TI) is presented. The closed form technique gives practically the same complex weights as the PWS optimization technique for large ring radius case. The proposed technique shows that the impact of the antenna pattern on the received voltage accuracy is ruled by Nyquist sampling

Wei Fan, Jesper Ø. Nielsen, Ondrej Franek, and Gert F. Pedersen are with the Antennas, Propagation and Radio Networking section at the Department of Electronic Systems, Faculty of Engineering and Science, Aalborg University, Denmark (email: {wfa, fs, jni, gfp}@es.aau.dk).

Xavier Carreño, Jagjit S. Ashta, and Mikael B. Knudsen are with Intel Mobile Communications, Denmark (email: {xavier.carreno, jagjitx.singh.ashta, mikael.knudsen}@intel.com).

theory.

- The impact of the antenna pattern on emulation accuracy for spatial correlation of the received signals in the PFS method is demonstrated by simulation and measurement results.
- We show that to test realistic DUTs with higher variations in directivity, we need more probes to maintain the same received voltage and spatial correlation accuracy level.

II. Method

A. Plane wave synthesis technique

In this section, we describe the optimization techniques to generate a single static plane wave with an arbitrary direction impinging the test area for both vertical and horizontal polarization. Note that the PWS technique for vertical polarization has been addressed in several contributions and the same notations as in [2] has been adopted in this paper. The main contribution of this part lies in two aspects: the optimization problem is formed as a convex optimization problem, which gives optimal results and low complexity; an optimization technique for PWS of the horizontal polarization is introduced.

1) Vertical polarization : As shown in Figure 1, a target plane wave is with an arbitrary direction $\overline{\beta}_{AoA}$ impinging the test area. $\overline{\beta}_{AoA}$ is a wave vector with $\parallel \overline{\beta}_{AoA} \parallel = \frac{2\pi}{\lambda}$. We approximate the target plane wave inside the test area by superposing the radiated fields from each of the OTA probes. Complex weights are obtained by minimizing the difference between the target field and the synthesized field within the test area. One constraint with the practical system is that probe weights are limited, as the output gain of typical channel emulators is limited to 0 dB. The weighting vector $\boldsymbol{g_\theta}$ for a vertically polarized single plane wave can be obtained by solving the optimization problem as follows:

$$\min_{\boldsymbol{g_\theta}} \ \|\mathbf{F}_\theta \boldsymbol{g_\theta} - \boldsymbol{t}_\theta\|_2^2 \qquad (1)$$
$$\text{s.t.} \quad 0 \le |g_{\theta,k}| \le 1 \ \forall k \in [1, K]$$

where

- $||\cdot||_2$ denotes the second order norm.
- $\boldsymbol{g_\theta} = \{g_{\theta,k}\} \in \mathbb{C}^{K\times 1}$ is a vector of the complex weights for vertically polarized probes. K is the number of probes.
- $\boldsymbol{t}_\theta = \{e(\overline{r}_m)\} \in \mathbb{C}^{M\times 1}$ is a vector of vertically polarized complex target field samples. M is the total number of sample points. $\overline{r}_m$ is a position vector of sample point m.
- $\mathbf{F}_\theta = \{f(m,k) \in \mathbb{C}^{M\times K}\}$ is a transfer matrix of known gains from the probes to the sample points.

The target field for an ideal plane wave is with uniform power distribution and linear phase front along the propagation direction, that is,

$$e(\overline{r}_m) = E_0 \exp(-j\overline{\beta}_{AoA} \cdot \overline{r}_m), \qquad (2)$$

where the field strength E_0 is assumed constant and $(\cdot)$ is the dot product operator. The transfer coefficient from the kth OTA antenna to the mth location $\overline{r}_m$ is:

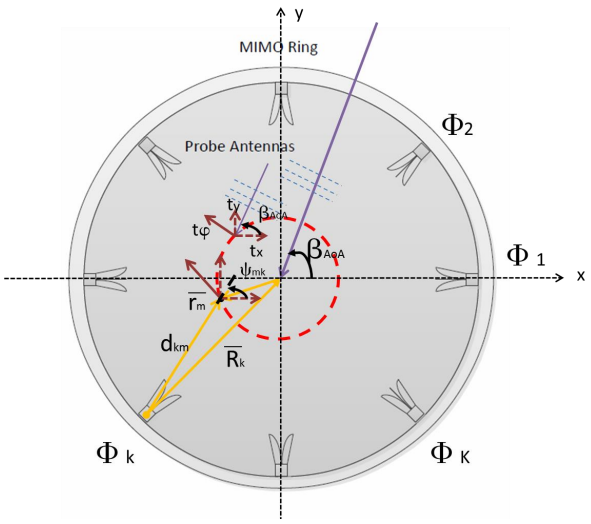

Figure 1. A single plane wave with AoA β_{AoA} impinging the test area.

$$f(m,k) = A(d_{km}) \cdot \exp(-j\frac{2\pi}{\lambda} d_{km}), \qquad (3)$$

where $d_{km} = \parallel \overline{d}_{km} \parallel = \parallel \overline{R}_k + \overline{r}_m \parallel$ is the distance from the kth OTA antenna to the mth location. $A(d_{km})$ is the free space path loss factor. $\overline{R}_k$ is a position vector of the kth probe.

2) Horizontal polarization: The same principle can be applied for the horizontal polarization:

$$\min_{\boldsymbol{g_\varphi}} \ \|\mathbf{F}_\varphi \boldsymbol{g_\varphi} - \boldsymbol{t}_\varphi\|_2^2, \qquad (4)$$

where $\boldsymbol{g_\varphi} = \{g_{\varphi,k}\} \in \mathbb{C}^{K\times 1}$, $\boldsymbol{t}_\varphi \in \mathbb{C}^{M\times 1}$ and $\mathbf{F}_\varphi \in \mathbb{C}^{M\times K}$ are defined similarly to the vertical polarization.

The PWS technique for vertical and horizontal polarizations is addressed in [4], [10], [11]. In a 2D MIMO OTA setup as illustrated in Figure 1, the direction of the vertically polarized field will be perpendicular to the xy (azimuth) plane both for the emulated and target fields. However, for the horizontally polarized field, the direction of the target field is on xy plane and perpendicular to the AoA of the target plane wave, while the direction of the radiated field from a horizontally polarized probe is on the xy plane and perpendicular to the AoA from where the probe is located. That is, the direction of the target field and emulated field might be different. In order to ensure that the emulated field matches with the target field in terms of magnitude, phase, and polarization for the sample points inside test zone, decomposition into the two orthogonal axises x and y is required for the horizontal polarization. This effect is, however, not considered in the literature so far.

We can decompose the target field and the transfer matrix into x and y orthogonal components, as:

- $\mathbf{F}_x = \{f_x(m,k)\} \in \mathbb{C}^{M\times K}$ with $f_x(m,k) = -f(m,k) \cdot \sin(\psi_{mk})$
- $\mathbf{F}_y = \{f_y(m,k)\} \in \mathbb{C}^{M\times K}$ with $f_y(m,k) = f(m,k) \cdot \cos(\psi_{mk})$
- $\boldsymbol{t}_x = \{e_x(\overline{r}_m)\} \in \mathbb{C}^{M\times 1}$ with $e_x(\overline{r}_m) = -e(\overline{r}_m) \cdot \sin(\beta_{AoA})$

- $\boldsymbol{t}_y = \{e_y(\overline{r}_m)\} \in \mathbb{C}^{M\times 1}$ with $e_y(\overline{r}_m) = e(\overline{r}_m) \cdot \cos(\beta_{AoA})$

where β_{AoA} is the AoA of the target plane wave and ψ_{mk} is angle between $\overline{d}_{km}$ and x axis, as illustrated in Figure 1.

Then the objective function to obtain the optimal weights for horizontal polarization can be rewritten as:

$$\min_{\mathbf{g}_{\boldsymbol{\varphi}}} \left\| \begin{bmatrix} \mathbf{F}_x \\ \mathbf{F}_y \end{bmatrix} \boldsymbol{g}_{\boldsymbol{\varphi}} - \begin{bmatrix} \boldsymbol{t}_x \\ \boldsymbol{t}_y \end{bmatrix} \right\|_2^2 \quad \text{s.t.} \quad 0 \le |g_{\varphi,k}| \le 1 \; \forall k \in [1, K] \tag{5}$$

Both objective functions in equation (1) and (5) are quadratic programming problems with linear constraints. This standard convex optimization problem can then be solved using the cvx package in Matlab with high efficiency [12].

B. Equivalent induced voltage (EIV) technique

For the PWS technique, the goal is to generate the plane waves with arbitrary AoAs impinging the test area. However, what matters is the difference between the induced received voltage, with waves radiated from the probes and the target received voltage, with ideal impinging plane waves. The induced received voltage accuracy will depend on the field synthesis accuracy and the DUT antenna pattern. The goal of the EIV technique is to obtain the complex weights such that the target received voltage with an arbitrary impinging plane wave can be reproduced with the multiple probes.

The antenna radiation pattern is defined as a complex function of direction, whose value gives the intensity of the radiated field in the far field area. Due to the reciprocity theorem, the same complex function gives us the voltage on the antenna terminals depending on from which direction an ideal plane wave is impinging to the antenna. The received voltage can be represented as

$$V = E_0 \cdot L(\alpha). \tag{6}$$

If the electric intensity of the incident field E_0 is constant, then the induced voltage V varies with the AoA α of the plane wave according to the radiation pattern L. L also represents the effective length of an antenna.

In a multi-probe anechoic chamber OTA setup as shown in Figure 1, the OTA ring radius $R = ||\overline{R}_k||$ is much larger than the DUT and ideal plane waves radiating from the probes are assumed. The resulting received voltage at the antenna terminal will be given by the superposition of the partial voltages which corresponds to antenna pattern sampled at the discrete angles in which the OTA probes are placed:

$$\hat{V} = \sum_{k=1}^{K} V_k = E_0 \cdot \sum_{k=1}^{K} g_k(\alpha) L(\Phi_k) = E_0 \cdot \hat{L}(\alpha), \tag{7}$$

where $g_k(\alpha)$ is the complex weight assigned for the kth probe. Φ_k is the angular location of kth probe. $\hat{L}(\alpha)$ is the resulting value of the antenna pattern at arbitrary direction α, given by a summation of the samples of antenna pattern at the directions of the probes, weighted by the complex weights. To ensure to we obtain $\hat{V} = V$, we need to find $\boldsymbol{g(\alpha)}$ so that we have $L(\alpha) = \hat{L}(\alpha)$ for an arbitrary direction α. This can be seen as an antenna pattern interpolation problem, where we need to reconstruct the antenna pattern $L(\alpha)$ from K discrete periodic samples $L(\Phi_k)$.

We assume the probes are located on the OTA ring with equal spacing between them,

$$\Phi_{K,k} = \frac{360^o}{K}(k-1). \tag{8}$$

The antenna pattern $L(\alpha)$ sampled by K equidistant probes is a periodic (with the period 2π) sequence. The EIV problem can be solved by TI, as stated below.

1) Trigonometric interpolation: Let us describe the interpolation of the radiation pattern as

$$\hat{L}(\alpha) = \sum_{k=1}^{K} g_k(\alpha) L(\Phi_k) \tag{9}$$

where α is the azimuth angle of the plane wave. The weights of the probes $g_k(\alpha)$ can then be expressed, using trigonometric interpolation [13], as

$$g_k(\alpha) = \frac{1}{K} \sum_{k=1}^{K} \cos m(\alpha - \Phi_k), \tag{10}$$

with $m = k - \lceil N/2 \rceil$, where $\lceil \rceil$ is the ceiling operator which rounds up the number inside the bracket to the next higher integer.

If the phase at the ring center is set to 0. The complex weights for interpolation is:

$$g_{TI,k}(\alpha) = g_k(\alpha) \exp(-j\beta R) \tag{11}$$

where β is the wave number. Note that the complex weights are independent of the antenna pattern samples $L(\Phi_k)$ and plane wave polarizations.

In this part, ideal plane waves radiating from the probes are assumed. Also, uniform probe configuration on the OTA ring is assumed for the sake of simplicity. The TI used for EIV technique detailed here can be extended to the case where OTA probes are not uniformly located on the OTA ring [13]. The TI can also be extended to 3D MIMO OTA configurations.

2) Antenna pattern impact on the EIV technique: According to the Nyquist sampling criterion, the number of probes K for complete reconstruction of the antenna pattern $L(\alpha)$ must exceed two times the highest harmonics in the spatial frequency spectrum of the antenna pattern. We expect to have certain conditions on smoothness of the antenna pattern versus density of number of probes. That is, if the antenna pattern variation is too high with respect to the number of probes, K will not satisfy the Nyquist criterion. As a result, the resulting interpolated values will present aliasing. An example is shown in Figure 2, where $K = 8$ uniformly located probes are used to sample the antenna pattern. However, since the antenna pattern variation is too high with respect to the number of probes, the interpolated antenna pattern $\hat{L}$ is different from the original antenna pattern L. As a result, the resulting received voltage $\hat{V}$ will not be the same as the target received voltage V for some AoAs. More probes are required to obtain the correct induced received voltage.

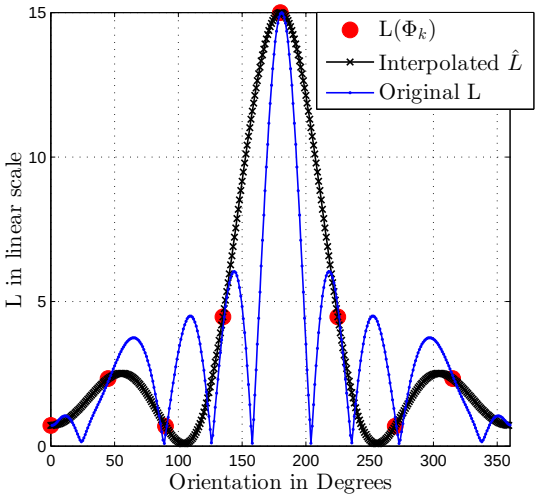

Figure 2. An illustration of inaccurate interpolated antenna pattern.

3) Required number of probes for the EIV technique : The antenna radiation pattern of any antenna with a fixed size (inside a limited test volume) can be described with a finite series of spherical wave functions [14]. That is, the highest harmonics in the spatial frequency spectrum of the antenna pattern is limited. The antenna pattern $L(\alpha)$ is thus a band-limited periodic function, which can be perfectly reconstructed with a finite number of probes. The highest significant wave mode present is given by [14],

$$K_{mode} = \lceil kr_t + 10 \rceil, \tag{12}$$

where r_t is the radius of the minimum spherical volume that contains the DUT. The minimum number of required probes for the complete reconstruction of $L(\alpha)$, according to Nyquist criterion is [14]:

$$K_{min}^{2D} = 2K_{mode} + 1, \tag{13}$$

where the superscript $2D$ refers to the 2D MIMO OTA configurations.

C. Prefaded signal synthesis technique

A channel model specifies a certain continuous power azimuth spread (PAS) at the Rx. However, with a limited number of probes, we can only approximately reproduce the PAS inside the test area. Spatial correlation has been selected as the main figure of merit (FoM) to characterize the channel spatial information at receiver side [2], [6]–[9], [15]. Omnidirectional antenna patterns are used for the channel emulation purpose as the DUT antenna pattern is typically not known beforehand. Furthermore, if some antenna patterns are embedded to the channel model, the channel model itself will assume some DUT antennas. Thus, it is not realistic to use the emulated channel to evaluate the DUT performance [7], [8].

As explained in [2], The PFS technique works the same for both vertically and horizontally polarized PAS. The theoretical spatial correlation between a pair antenna elements can be determined according to [16]:

$$\rho_a = \frac{\int_{-\pi}^{\pi} G_u(\phi) G_v^{\star}(\phi) p(\phi) d\phi}{\sqrt{\int_{-\pi}^{\pi} p(\phi)|G_u(\phi)|^2 d\phi}\sqrt{\int_{-\pi}^{\pi} p(\phi)|G_v(\phi)|^2 d\phi}} \tag{14}$$

where G_u and G_v are the complex radiation patterns of antennas u and v, respectively, with a common phase center. $p(\phi)$ is the PAS. In order to be used as an angular power density function, the $p(\phi)$ needs to satisfy $\int_{-\pi}^{\pi} p(\phi)d\phi = 1$. Using this property and the omnidirectional antenna pattern assumption, we can rewrite (14) as:

$$\rho = \int_{-\pi}^{\pi} \exp(j\beta(\overline{r}_u - \overline{r}_v) \cdot \overline{\phi}) p(\phi) d\phi \tag{15}$$

where $\overline{r}_u$ and $\overline{r}_v$ are vectors containing the position information of antenna u and v, respectively. $\overline{\phi}$ is an unit vector corresponding to the azimuth angle ϕ.

The goal is to obtain OTA probe power weights which minimize the deviation between the theoretical spatial correlation resulting from the target continuous PAS, and the emulated correlation resulting from the discrete PAS characterized by the power weights of the probes. Similar to (15), the emulated spatial correlation can be calculated based on the discrete PAS as:

$$\hat{\rho} = \sum_{k=1}^{K} w_k \exp(j\beta(\overline{r}_u - \overline{r}_v) \cdot \overline{\Phi}_k), \tag{16}$$

where w_k is the power weight for the kth probe. $\overline{\Phi}_k$ is a unit position vector of the kth probe. Optimization techniques to obtain power weights $\boldsymbol{w} = \{w_k\} \in \mathbb{R}^{K\times 1}$ have been discussed in [2], [7], [8] and results from [7] are used here.

Once the optimal power weights vector $\boldsymbol{w}$ is found, the resulting spatial correlation with antenna pattern $\hat{\rho}_a$ can be written as:

$$\hat{\rho}_a = \frac{\sum_k G_u(\theta_k) \cdot G_v^*(\Phi_k) \cdot w_k}{\sqrt{\sum_k |\, G_u(\Phi_k)\,|^2\, w_k \cdot \sum_k |\, G_v(\Phi_k)\,|^2\, w_k}}, \tag{17}$$

where G_u and G_v can be obtained through electromagnetic antenna simulations or measurements in an anechoic chamber.

The deviation between $\hat{\rho}$ and ρ shows how well the channel PAS is reconstructed, and hence it is generally selected as FoM to investigate the relationship between the number of required probes and test area size [2], [7]–[9], [17]. However, this does not take into account the DUT antenna pattern and what really matters is the deviation between target correlation ρ_a and emulated spatial correlation $\hat{\rho}_a$ with antenna patterns. In this paper, the focus is on the impact of antenna pattern on deviation between ρ_a and $\hat{\rho}_a$.

III. MIMO OTA MEASUREMENT

A. Introduction

An illustration of a general multi-probe anechoic chamber setup is shown in Figure 3. In the measurement of

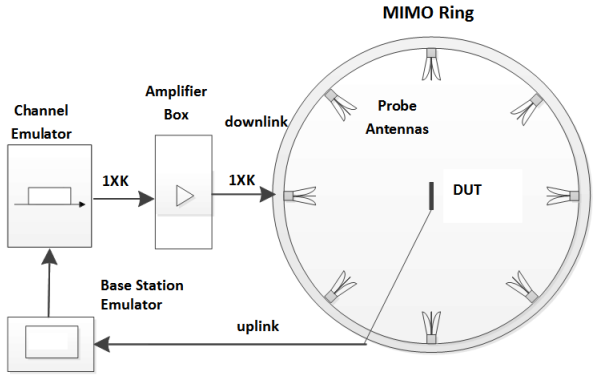

Figure 3. An illustration of the multi-probe based MIMO OTA setup. The main components are a base station emulator (BSE), one or several radio channel emulators, an anechoic chamber, OTA probe antennas, power amplifiers (PAs) and an DUT.

the current work, the BSE is replaced by a vector network analyzer (VNA). Figure 4 shows the multi-probe setup used for measurements at Aalborg University. 16 dual polarized horn antennas are equally spaced and fixed on an aluminum OTA ring with radius $R = 2$ meters.

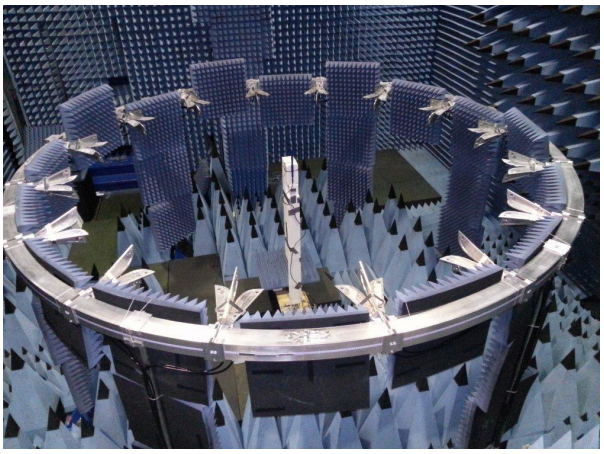

Figure 4. An illustration of the practical anechoic chamber setup in the measurement system.

B. Measurement setup for PFS

1) System setup : The PFS measurement setup is summarized in Table I.

2) Test DUTs and test channel scenarios: Since the paper aims at investigating the antenna pattern impact, special attention has been paid to selecting DUTs.

a) Test DUTs: Three test DUTs were used for the measurements: a pair of practical dipoles with antenna separation 0.525λ (at frequency 2100MHz) (shown in Figure 5(a)), the CTIA band 7 good antenna (shown in Figure 5(b)) and the CTIA band 7 nominal antenna (shown in Figure 5(c)) both with antenna separation 0.5λ (at frequency 2655MHz). The CTIA reference antennas are used to rule out the measurement uncertainty introduced by antenna patterns between different labs [18]. The so-called "good" antennas were designed

Table I
SETUP AND SPECIFICATIONS FOR THE PFS MEASUREMENTS

Component	Setup and specifications
VNA	Sweep time: 4.803s Number of sweeps per DUT orientation: 13 Number of samples per sweep: 1601
Channel emulator	A radio channel (implementation method detailed in [2]) with following parameter sets: • 10000 channel impulse responses (CIRs) are created and stored. • The CIRs are mapped to the OTA probes with the PFS algorithm implemented in the Elektrobit Propsim channel emulator.
Turntable	The DUT is rotated 360^o with 4^o step size for test scenario A and B and 5^o step size for test scenario C and D listed in Table II.
OTA probes	Only vertical polarization is considered.

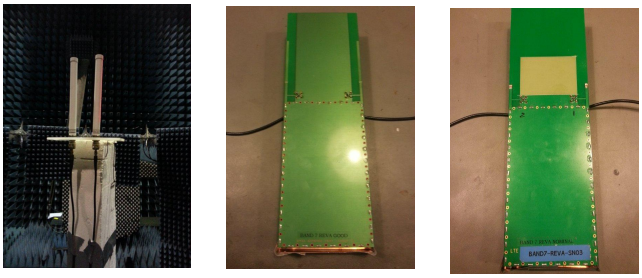

(a) Two practical dipoles (b) CTIA band 7 good (c) CTIA band 7 nominal

Figure 5. DUTs used in the measurements

to emulate good MIMO antenna systems that present low correlation coefficient, high total antenna efficiency and low gain imbalance, while the "nominal" antennas present median correlation coefficient, median total antenna efficiency and low gain imbalance. Note that the CTIA reference antennas were designed for the isotropic incoming power distribution only. The correlation coefficient in this work will depend on how the antennas are placed and the specific incoming power distribution. All three DUTs are vertically placed with respect to the OTA ring (as shown in Figure 5(a) and Figure 6(a)).

Mobile terminals could be arbitrarily positioned by the end users in real life and the antenna pattern in certain orientations can be critical compared to that in vertical positions. CTIA antennas are slanted 45^o in the measurements as well, as shown in Figure 6(b). Note that the DUT positions were carefully calibrated to ensure that the center of the two antennas on the DUT match with the center of the OTA ring and the rotation center of the turntable for all the measurements as shown in Figure 6(a) and Figure 6(b).

b) Test Scenarios: For the sake of simplicity, single clusters with Laplacian shaped PAS are considered as the target channels. Various AoAs and azimuth spread (AS) of 35^o are used to characterize the considered target clusters. AS = 35^o is selected as the standard channel models, e.g. the 3GPP spatial channel model extended (SCME) models, which have been considered as the target channel models in the MIMO OTA setup, are with AS = 35^o for the clusters [1],

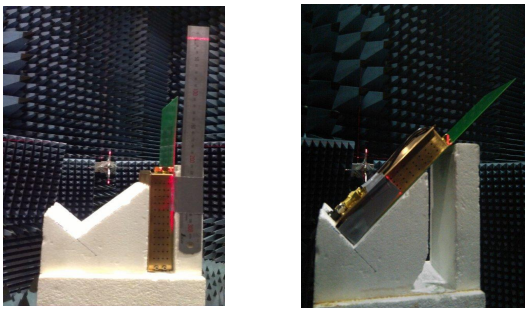

(a) Vertically positioned CTIA anenna

(b) 45 degrees slanted CTIA anenna

Figure 6. An illustration of DUT position calibrations with a laser positioner

Table II
TEST SCENARIOS

Scenario	Comments
A	AoA = 0^o and AS = 35^o Number of probes: 8
B	AoA = 22.5^o and AS = 35^o Number of probes: 8
C	AoA = 0^o and AS = 35^o Number of probes: 16
D	AoA = 22.5^o and AS = 35^o Number of probes: 16

[19], [20]. Four test scenarios are emulated with the channel emulators as listed in Table II. One channel emulator and 8 probes were used to emulate scenario A and B, while two channel emulators and 16 probes were used for scenario C and D. Only vertical polarization is considered.

3) Measurement procedure: For each DUT, complex radiation patterns of the two antenna elements are measured with the VNA at the same time with 1 degree resolution. Correlation measurements are performed for each test scenario with the same setup just after the antenna pattern measurements to ensure that the radiation patterns of the DUT remain unchanged for the correlation measurements. The VNA sweep time is selected according to the maximum Doppler shift defined in the test scenarios to meet the Nyquist sampling criterion.

The measured spatial correlation at DUT orientation ϕ_a is calculated according to the correlation definition:

$$\rho_m(\phi_a) = \frac{\sum_{i=1}^{I}(s_u(i) - s_{u,m})(s_v(i) - s_{v,m})}{\sqrt{\sum_{i=1}^{I}(s_u(i) - s_{u,m}).\sum_{i}^{I}(s_v(i) - s_{v,m})}} \quad (18)$$

where $s_u(i)$ and $s_v(i)$ are the ith complex signals received at antenna element u and v , respectively, at the antenna orientation index ϕ_a. $s_{u,m}$ and $s_{v,m}$ are the mean received signal over all measured samples for the two antennas, respectively.

IV. RESULTS AND DISCUSSION

A. Comparison between the PWS and the EIV technique

As mentioned previously, the goal of the PWS technique is to obtain complex weights to create plane waves impinging the test area, while the EIV technique is used to obtain complex weights to reproduce the target received voltage with arbitrary impinging plane waves. In this part, we will first show the complex weights obtained by the two techniques. After that the relationship between the two techniques is described. In the end, we will show the pros and cons of each technique.

The real and imaginary part of the complex weighting matrix $\boldsymbol{G}_{TI}$ obtained with the EIV technique with $R = 2$m and $f = 2.45$GHz is shown in Figure 7. The plots show the real and imaginary parts of a 360×8 complex weighting matrix with the ith row containing the 8 complex weights for the EIV at angle $\alpha = (i-1)^o$. The periodic pattern observed in Figure 7 is with period 45^o due to the symmetry of the probe configuration. The complex weighting matrix $\mathbf{G}_{\theta,op}$ and $\boldsymbol{G}_{\phi,op}$ are used to represent the complex weighting matrix obtained for vertically and horizontally polarized plane waves with AoA ranges from 0^o to 359^o with 1^o step, respectively. The difference between $G_{\theta,op}$ and $G_{\phi,op}$ for $R = 0.5$m, $R = 2$m, $R = 1000$m is shown in Figure 8 (figures on the left). The difference depends on the ratio between test area radius and ring radius r/R. Simulation results show that complex weights for the two polarizations are practically the same for $R \geqslant 2$ meters, which is consistent with the fact that the complex weights obtained with the EIV technique is independent of polarizations.

The difference between $\mathbf{G}_{TI}$and $\boldsymbol{G}_{\phi,op}$ for $R = 0.5$m, $R = 2$m, $R = 1000$m is shown in Figure 8 (figures on the right). The difference between the two complex weighting matrix is due to the limited ring radius. As explained in Section II-B, ideal plane waves radiating from the probes are assumed. The complex weighting matrix obtained with the EIV technique is practically the same as the weights obtained with the PWS optimization technique for large R case. The conclusion for relationship between test area size and number of probes is consistent for the PWS and the EIV techniques. For the PWS technique, the smaller the test area, the smaller number of required probes we need to maintain the field synthesized accuracy. For the EIV technique, the smaller the test area, the smaller number of required probes we need to reconstruct the received voltage. Note that for a multi-probe setup with $R \geqslant 2$m, complex weighting matrix $\mathbf{G}_{TI}$, $\boldsymbol{G}_{\phi,op}$ and $\mathbf{G}_{\theta,op}$ are practically the same.

Depending on the number of samples selected for field synthesis and the number of plane waves for optimization, the PWS can be computationally heavy. While the EIV technique offer a closed form solution for large R case. However, for small R cases, the PWS technique offer better accuracy. Furthermore, accurate field synthesis is not sufficient to guarantee accurate resulting received voltage. The received voltage accuracy depends on the DUT antenna pattern, which can not be demonstrated by the PWS technique.

Measurement verification of the PWS technique is given in [5]. Good agreement between measurements and simulations has been achieved in terms of the received voltage, as an omnidirectional Satimo calibration dipole was used as the DUT.

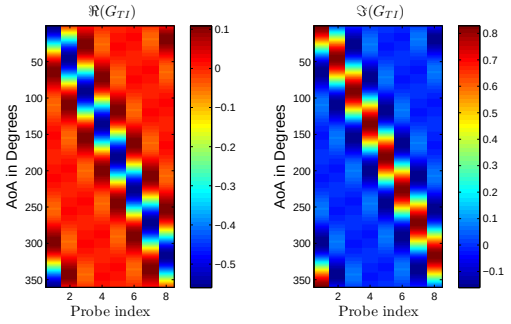

Figure 7. Real and imaginary part of the complex weighting matrix G_{TI} with TI technique for $R = 2$m. The phase at the ring center is set to 0 the frequency is set to 2.45GHz.

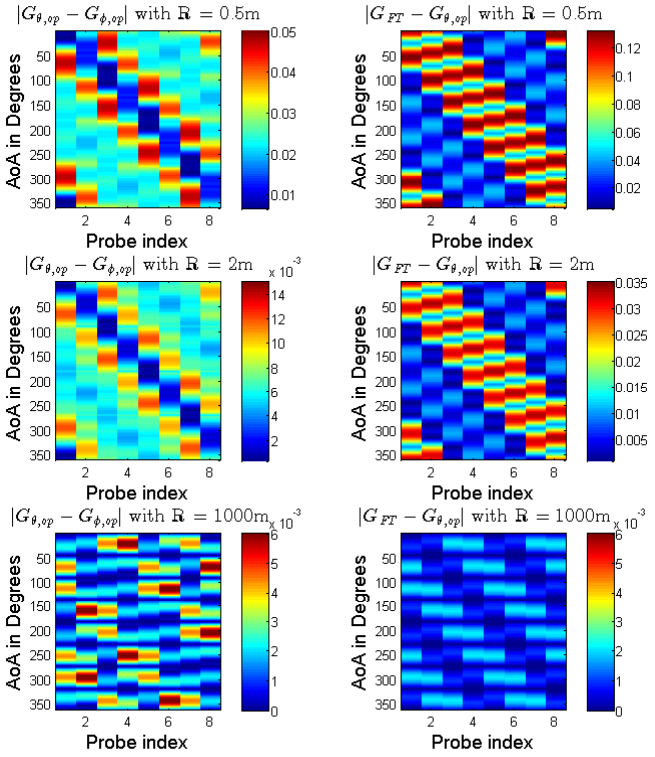

Figure 8. Difference between $G_{\theta,op}$ and $G_{\phi,op}$ and difference between $G_{\theta,op}$ and G_{TI} for $R = 0.5$m, $R = 2$m, $R = 1000$m respectively. The phase at the ring center is set to 0. The frequency is set to 2.45GHz and test area radius $r = 0.35\lambda$ is selected for the PWS optimization.

B. Results for prefaded signal synthesis (PFS)

1) Measured radiation pattern results: The measured radiation patterns of the DUTs are shown in Figure 9 and Figure 10. Due to the close-by antenna coupling impact, the dipole gain patterns are not omnidirectional. The measured phase patterns of the practical dipoles, vertically placed CTIA good and nominal antennas over DUT orientation follow sinusoidal curves quite well, as shown in Figure 9. However, the measured phase patterns of 45^o slanted CTIA good and nominal antennas do not follow sinusoid curves at all (not shown). Phase patterns are quite inaccurate when the gain patterns are in deep fades. Deep nulls are present in the

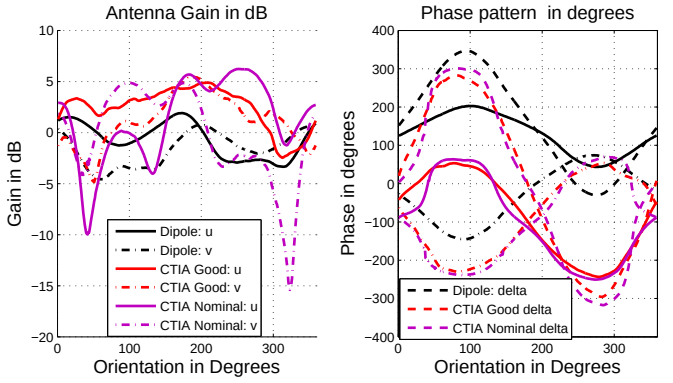

Figure 9. Measured antenna patterns for practical dipoles, vertically placed CTIA good and nominal antennas. Legend delta in the phase pattern curves corresponds to the phase difference between u and v. Note that the power amplifier gain, cable and free space propagation attenuation are not normalized in the results.

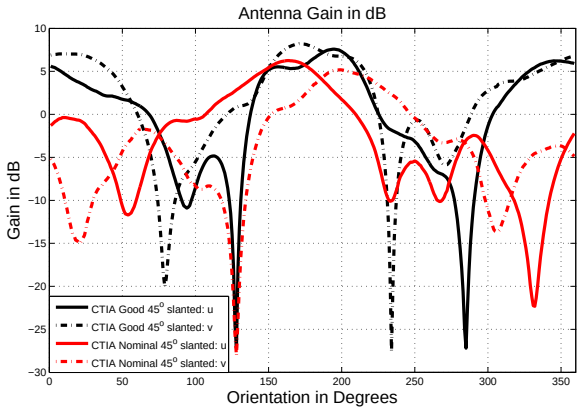

Figure 10. Measured antenna patterns for the 45^o slanted CTIA good and nominal antennas.

gain patterns for the two DUTs, as shown in Figure 10. The measured antenna pattern are used to calculate ρ_a and $\hat{\rho}_a$ as specified in (14) and (17), respectively.

2) Emulated spatial correlation results: Table III summarizes the spatial correlation emulation error $|\rho_a - \hat{\rho}_a|$ for all the DUTs in the four test scenarios. The ideal DUT denotes two omnidirectional antennas with 0.5λ antenna separation. $|\rho_a - \hat{\rho}_a|$ for the practical dipoles present comparable accuracy when compared with ideal DUT case for all the test scenarios. However, the relative error level is higher for practical dipoles, as correlation over orientations for the ideal DUT ranges from 0.25 to 0.8, compared with from 0.45 to 0.7 for the practical dipoles, as shown in Figure 11.

$|\rho_a - \hat{\rho}_a|$ in the test scenario A present better accuracy than in B for all the DUTs. This is expected since the test area performance is the best if the cluster is arriving to the test area from the direction where one of the OTA antennas are located (Scenario A), while the worst case is the cluster impinging from an angle exactly in the middle of two adjacent OTA probes (Scenario B). Emulation results in test scenario C and D present comparable accuracy. Test area emulation accuracy highly depends on the number of probes used in the setup.

Table III
STATISTICS OF SPATIAL CORRELATION EMULATION ERROR $|\rho_a - \hat{\rho}_a|$ AND STATISTICS OF MEASURED CORRELATION DEVIATION FROM EMULATED CORRELATION $|\rho_m - \hat{\rho}_a|$ FOR ALL TEST SCENARIOS

Test DUT	A				B				C				D			
	$\lvert\rho_a - \hat{\rho}_a\rvert$		$\lvert\rho_m - \hat{\rho}_a\rvert$		$\lvert\rho_a - \hat{\rho}_a\rvert$		$\lvert\rho_m - \hat{\rho}_a\rvert$		$\lvert\rho_a - \hat{\rho}_a\rvert$		$\lvert\rho_m - \hat{\rho}_a\rvert$		$\lvert\rho_a - \hat{\rho}_a\rvert$		$\lvert\rho_m - \hat{\rho}_a\rvert$	
	rms	max	rms	max	rms	max	rms	max	rms	max	rms	max	rms	max	rms	max
Ideal DUT	0.03	0.05			0.10	0.15			0.01	0.01			0.01	0.01		
Dipoles	0.04	0.07	0.04	0.06	0.09	0.14	0.05	0.08	0.01	0.02	0.02	0.05	0.01	0.02	0.03	0.04
Nominal	0.11	0.18	0.02	0.05	0.22	0.33	0.03	0.05	0.01	0.03	0.04	0.08	0.02	0.04	0.04	0.08
Good	0.16	0.28	0.03	0.05	0.29	0.45	0.06	0.14	0.02	0.04	0.05	0.10	0.02	0.05	0.08	0.20
Nominal slanted	0.20	0.44	0.09	0.34	0.30	0.53	0.08	0.15	0.02	0.03	0.07	0.11	0.03	0.05	0.11	0.32
Good slanted	0.29	0.61	0.09	0.18	0.38	0.71	0.05	0.12	0.02	0.04	0.08	0.15	0.04	0.08	0.07	0.13

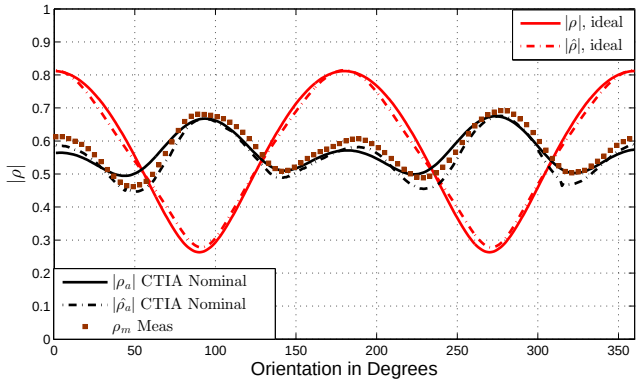

Figure 11. Target $|\rho_a|$, emulated $|\hat{\rho}_a|$ and measured $|\rho_m|$ spatial correlation for practical dipoles for test scenario A.

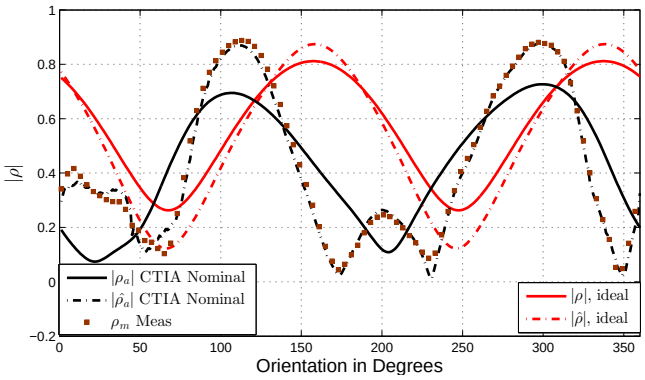

Figure 12. Target $|\rho_a|$, emulated $|\hat{\rho}_a|$ and measured $|\rho_m|$ spatial correlation for the vertically placed CTIA good antenna for test scenario B.

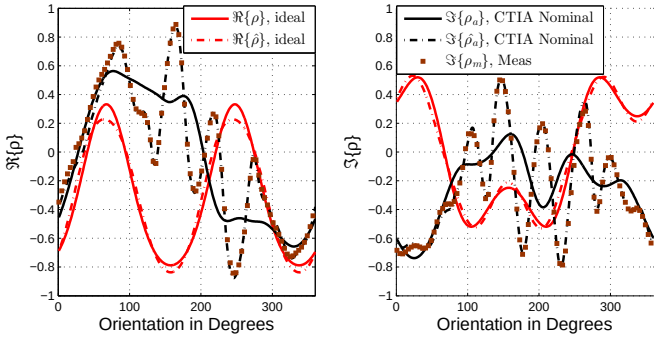

Figure 13. Real and imaginary part of the target ρ_a, emulated $\hat{\rho}_a$ and measured ρ_m spatial correlation for the 45^o slanted placed CTIA good antenna for test scenario B.

Therefore, emulation accuracy results in scenario C and D are much better than in A and B for all the DUTs, respectively.

For test scenario A and B, the antenna patterns have a great impact on emulation accuracy. Maximum emulation error is 0.15 for the ideal DUT for test scenario B and up to 0.71 for the 45^o slanted CTIA good antenna. Figure 12 shows the target, emulated and measured spatial correlation for the vertically placed CTIA good antenna for test scenario B. The root mean square (RMS) emulation error $|\rho_a - \hat{\rho}_a|$ is 0.29, although $|\hat{\rho}_a|$ follows the tendency of $|\rho_a|$ very well over orientations. Figure 13 shows the real and imaginary part of the target, emulated and measured spatial correlation for the 45^o slanted CTIA good antenna for test scenario B. Although both the real and imaginary part of $\hat{\rho}_a$ follow the tendency of ρ_a, big deviations exist. If the antenna pattern variation is too high with respect to the number of probes, $\hat{\rho}_a$ will be inaccurate. The antenna pattern hence have to be considered when investigating the required number of OTA probes. The antenna pattern impact on spatial correlation emulation accuracy in test scenario C and D is negligible. As shown in Figure 14, both the real and imaginary parts of $\hat{\rho}_a$ follow ρ_a accurately for the 45^o slanted CTIA nominal antenna for test scenario C.

3) Measurement results: Statistics of the deviation between the measured correlations from the emulated correlations $|\rho_m - \hat{\rho}_a|$ for all the DUTs in all test scenarios are shown in Table III. Measurement verification of the ideal DUT with a virtual uniform linear array (ULA) can be found [17]. Measured spatial correlation ρ_m for all scenarios generally matches $\hat{\rho}_a$ accurately, as shown in Figure 11-14. RMS deviations of up to 0.05 can be found for the practical dipoles while the RMS deviation is up to 0.08 for vertically placed for the CITA good and nominal antennas. When placed 45^o slanted, very few big deviations can be found in some orientations for the CTIA antennas while the RMS deviation levels are only slightly higher than the vertically placed cases. Deviations are likely due to the cable movement. During the antenna pattern and correlation measurements, the cables that connect the DUT to the VNA are moving and bending around the turntable. Different cable movements may happen during the antenna pattern and correlation measurements, and hence the measured antenna patterns might be different from the antenna patterns that the DUT presents during the correlation measurements.

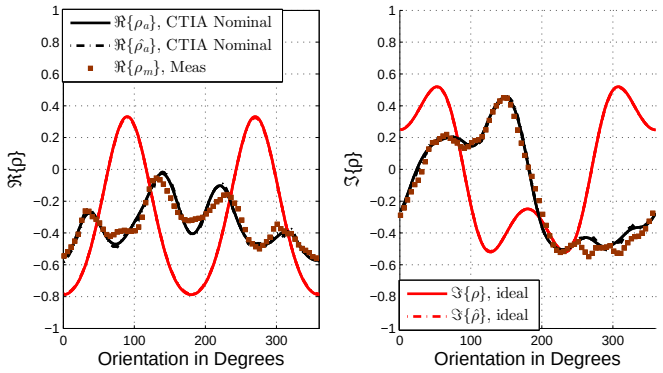

Figure 14. Real and imaginary part of the target ρ_a, emulated $\hat{\rho}_a$ and measured ρ_m spatial correlation for the 45^o slanted placed CTIA nominal antenna for test scenario C.

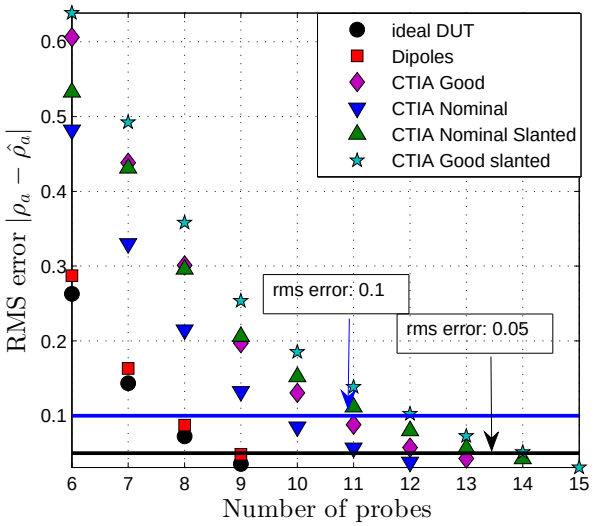

Figure 15. Number of required probes for realistic DUTs. Test zone size: 0.5λ.

4) Number of required probes for accurate spatial correlation reconstruction: Results have shown $|\rho_a - \hat{\rho}_a|$ depends on the target channel model. One criterion we should follow is that inside the test area, emulation accuracy should be sufficiently good even for the worst channel case. Figure 15 shows the number of required probes for realistic DUTs for a Laplacian shaped PAS with AoA =$180^o/K$ and AS = 35^o. The measured DUT radiation patterns are used to calculate $|\rho_a - \hat{\rho}_a|$ for a given number of probes. Figure 15 shows that we need only 8 probes for the dipoles within a test area size of 0.5λ with 0.05 rms error accuracy requirement. However, to obtain the same test area performance, we need as many as 14 probes for the 45^o slanted CTIA good antenna. The number of probes, which is considered enough to obtain accurate $|\rho - \hat{\rho}|$ for ideal DUTs [2], [7]–[9], [17], is generally not sufficient for realistic DUTs.

V. Conclusion

This paper investigates the impact of the antenna pattern on test zone performance for multi-probe based MIMO OTA setup from the received voltage and spatial correlation point of view. The PWS technique for horizontal polarization is introduced, and simulation results show that complex weights for the two polarizations are practically the same for large R. A novel closed form technique named the EIV technique to reproduce received voltage with arbitrary plane waves based on trigonometric interpolation is presented. The EIV technique presents practically the same complex weights as the PWS techniques for large R MIMO OTA setups. We have shown that the received voltage accuracy depends not only on the field synthesis accuracy, but also on the DUT radiation pattern. The impact of the antenna pattern on the received voltage accuracy is ruled by the Nyquist sampling theory. We show that more probes are required for DUTs with bigger variation in the antenna pattern to obtain accurate received voltage. Furthermore, in the PFS method, the impact of the antenna pattern on spatial correlation accuracy is investigated. Simulation and measurement results show that the number of probes, which is considered enough to obtain accurate spatial correlation $|\rho - \hat{\rho}|$ for ideal DUTs, is generally not sufficient for realistic DUTs with higher variation in the antenna pattern. For example, RMS emulation error for test scenario A with 8 uniformly spaced probes is 0.03 for the ideal DUTs for a test area of 0.5λ, while up to 0.29 for the 45^o slanted CTIA good antenna. We show that only 8 probes are sufficient to achieve 0.05 rms error accuracy for the dipoles within a test area size of 0.5λ. However, to obtain the same test area performance, we need as many as 14 probes for the 45^o slanted CTIA good antenna.

Wei Fan received his Bachelor of Engineering degree in electrical engineering from Harbin Institute of technology, China, in 2009 and Master's double-degree with highest honors from Politecnico di Torino, Italy, and Grenoble Institute of Technology, France, in electronic engineering in 2011. From February 2011 to August 2011, he was with Intel Mobile Communications, Denmark. He is currently a Ph.D. candidate at Department of Electronic Systems at Aalborg University, Denmark. His main areas of research are over the air testing of MIMO terminals and radio channel modeling.

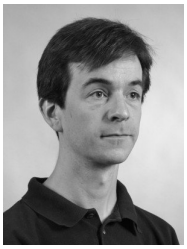

Jesper Ødum Nielsen received his master's degree in electronics engineering in 1994 and a PhD degree in 1997, both from Aalborg University, Denmark. He is currently employed at Department of Electronic Systems at Aalborg University where main areas of interests are experimental investigation of the mobile radio channel and the influence mobile device users have on the channel. He has been involved in MIMO channel sounding and modeling, as well as measurements using live GSM and LTE networks. In addition he has been working with radio performance evaluation, including over the air testing of active wireless devices.

Ondrej Franek was born in 1977. He received the M.Sc. (Ing., with honors) and Ph.D. degrees in electronics and communication from Brno University of Technology, Czech Republic, in 2001 and 2006, respectively. Currently, he is working at the Department of Electronic Systems, Aalborg University, Denmark, as an associate research professor. Since 2012, he has also been employed as an external consultant for antenna topics at Intel Mobile Communications in Aalborg, Denmark. His research interests include computational electromagnetics with focus on fast and efficient numerical methods, especially the finite-difference time-domain method. He is involved in research on antennas, biological effects of non-ionizing electromagnetic radiation, indoor and outdoor radiowave propagation, and electromagnetic compatibility.

Dr. Franek was the recipient of the Seventh Annual SIEMENS Award for outstanding scientific publication.

Xavier Carreño received his Master degree from 'Escola Tènica Superior d'Enginyeria de Telecomunicació de Barcelona' (UPC) in 2011. At UPC he was deeply involved in baseband signal processing algorithms and MIMO OTA research topics within Intel Mobile Communications, where he currently has a leading role in the MIMO OTA development team as system engineer. He is involved in the standardization of MIMO OTA methods and has coauthored several 3GPP, CTIA and IC1004 contributions and several conference and journal papers on the subject. His primary interests are within the area of MIMO OTA testing techniques, MIMO channel modeling and LTE platform testing.

Jagjit Singh Ashta born in 1988, obtained a Master Degree in Telecommunications in the 'Escola Tènica Superior d'Enginyeria de Telecomunicació de Barcelona' (UPC) in 2012. In the same year he completed with honours his Master Thesis on MAC layer improvements for IEEE 802.11 networks (WLAN) at Aalborg University (AAU) in collaboration with Nokia Solutions and Networks (NSN). Currently he develops his career as a Wireless Communications Engineer at Xtel ApS and is employed as an external software consultant at Intel Mobile Communications, Denmark. His research interests cover the MAC and PHY layers of the RANs and the development of software solutions required to study them.

Mikael Bergholz Knudsen was born in 1964. He received the B.S. degree in electrical engineering from Aarhus Teknikum, Denmark, in 1989, and the M.S. and Ph.D. degrees from Aalborg University, Denmark, in 1992 and 2001, respectively. In 1993, he joined Maxon Telecom A/S, Aalborg, Denmark, where he designed RF circuitry for both analog and digital mobile phones. From 1998 to 2001, he worked as an industrial Ph.D. student for Siemens Mobile Phones A/S, Denmark, while he at the same time studied at Aalborg University. He is now with Intel Mobile Communications Denmark, where he is the project manager for the 4th Generation Mobile Communication and Test platform (4GMCT) and also the chairman of the steering committee for the Smart Antenna Front End (SAFE) projects; both sponsored by the Danish National Advanced Technology Foundation. His areas of interest include RF system design and handset antenna performance including more than one antenna. In the resent years one of his focus areas has been how to utilize the unique possibilities in the cooperation between university researchers and private companies.

Gert Frølund Pedersen was born in 1965 and married to Henriette and have 7 children. He received the B.Sc. E. E. degree, with honour, in electrical engineering from College of Technology in Dublin, Ireland in 1991, and the M.Sc. E. E. degree and Ph. D. from Aalborg University in 1993 and 2003. He has been with Aalborg University since 1993 where he is a full Professor heading the Antenna, Propagation and Networking LAB with 36 researcher. Further he is also the head of the doctoral school on wireless communication with some 100 phd students enrolled. His research has focused on radio communication for mobile terminals especially small Antennas, Diversity systems, Propagation and Biological effects and he has published more than 175 peer reviewed papers and holds 28 patents. He has also worked as consultant for developments of more than 100 antennas for mobile terminals including the first internal antenna for mobile phones in 1994 with lowest SAR, first internal triple-band antenna in 1998 with low SAR and high TRP and TIS, and lately various multi antenna systems rated as the most efficient on the market. He has worked most of the time with joint university and industry projects and have received more than 12 M$ in direct research funding. Latest he is the project leader of the SAFE project with a total budget of 8 M$ investigating tunable front end including tunable antennas for the future multiband mobile phones. He has been one of the pioneers in establishing Over-The-Air (OTA) measurement systems. The measurement technique is now well established for mobile terminals with single antennas and he was chairing the various COST groups (swg2.2 of COST 259, 273, 2100 and now ICT1004) with liaison to 3GPP for over-the-air test of MIMO terminals. Presently he is deeply involved in MIMO OTA measurement.

REFERENCES

[1] M. Rumney, R. Pirkl, M. H. Landmann, and D. A. Sanchez-Hernandez, "MIMO Over-The-Air Research, Development, and Testing," *International Journal of Antennas and Propagation*, vol. 2012, 2012.

[2] P. Kyösti, T. Jämsä, and J. Nuutinen, "Channel modelling for multiprobe over-the-air MIMO testing," *International Journal of Antennas and Propagation*, 2012.

[3] P. Kyösti, J. Nuutinen, and T. Laitinen, "Over the air test," Patent WO 2012/117 147 A1, Sep. 7, 2012.

[4] T. Laitinen, P. Kyösti, J.-P. Nuutinen, and P. Vainikainen, "On the number of OTA antenna elements for plane-wave synthesis in a MIMO-OTA test system involving a circular antenna array," in *Antennas and Propagation (EuCAP), 2010 Proceedings of the Fourth European Conference on*. IEEE, 2010, pp. 1–5.

[5] W. Fan, X. Carreño, J. Ø. Nielsen, K. Olesen, M. B. Knudsen, and G. F. Pedersen, "Measurement Verification of Plane Wave Synthesis Technique Based on Multi-probe MIMO-OTA Setup," in *Vehicular Technology Conference (VTC Fall), 2012 IEEE*. IEEE, 2012, pp. 1–5.

[6] A. Khatun, H. Laitinen, V.-M. Kolmonen, and P. Vainikainen, "Dependence of Error Level on the Number of Probes in Over-the-Air Multiprobe Test Systems," *International Journal of Antennas and Propagation*, vol. 2012, 2012.

[7] P. Kyösti and J. Nuutinen, "Over the air test," Patent US 20 110 189 962, Aug. 4, 2011.

[8] J. D. Reed, "Emulation and controlled testing of MIMO OTA channels," Patent US 20 110 299 570, Dec. 8, 2011.

[9] M. A. Mow, B. Niu, R. W. Schlub, and R. Caballero, "Tools for design and analysis of over-the-air test systems with channel model emulation capabilities," Patent US 20 110 270 567, Nov. 3, 2011.

[10] J. Toivanen, T. Laitinen, V. Kolmonen, and P. Vainikainen, "Reproduction of Arbitrary Multipath Environments in Laboratory Conditions," *Instrumentation and Measurement, IEEE Transactions on*, vol. 60, no. 1, pp. 275–281, 2011.

[11] T. Laitinen and P. Kyösti, "On appropriate probe configurations for practical MIMO over-the-air testing of wireless devices," in *Antennas and Propagation (EUCAP), 2012 6th European Conference on*, 2012, pp. 1544–1548.

[12] S. Boyd and L. Vandenberghe, *Convex Optimization*. Cambridge University Press, 2004.

[13] G. Giacaglia, "Trigonometric interpolation," *Celestial mechanics*, vol. 1, pp. 360–367, 1970. [Online]. Available: http://dx.doi.org/10.1007/BF01231141

[14] J. E. Hansen, *Spherical near-field antenna measurements*. Peter Peregrinus Ltd, 1988, vol. 26.

[15] Y. Okano, K. Kitao, and T. Imai, "Impact of number of probe antennas for MIMO OTA spatial channel emulator," in *Antennas and Propagation (EuCAP), 2010 Proceedings of the Fourth European Conference on*. IEEE, 2010, pp. 1–5.

[16] R. Vaughan, J. Bach-Anderson, and J. B. Andersen, "Channels, propagation and antennas for mobile communications." Institution of Electrical Engineers, 2003.

[17] P. Kyosti, J.-P. Nuutinen, and T. Jamsa, "MIMO OTA test concept with experimental and simulated verification," in *Antennas and Propagation (EuCAP), 2010 Proceedings of the Fourth European Conference on*. IEEE, 2010, pp. 1–5.

[18] I. Szini, G. Pedersen, A. Scannavini, and L. Foged, "MIMO 2×2 reference antennas concept," in *Antennas and Propagation (EUCAP), 2012 6th European Conference on*, March, pp. 1540–1543.

[19] "Measurement of Radiated Perfromances for MIMO and Multi-antenna reception for HSPA, and LTE terminals," 3GPP/3GPP2, TR 37.976 v11.1.0, April. 2012.

[20] "Verification of radiated multi-antenna reception performance of User Equipment," 3GPP, TR 37.977 V0.2.0, May. 2012.